SURFACE RELIEF STRUCTURES FOR MULTIPLE BEAM LO GENERATION WITH HETERODYNING DETECTOR ARRAYS*

Wilfrid B. Veldkamp
Massachusetts Institute of Technology
Lincoln Laboratory
Lexington, Massachusetts 02173

SUMMARY

Linear and binary holograms have been developed for use in heterodyne detection with 10.6μm imaging arrays. These devices match the amplitude and phase of the local oscillator to the received signal and thus maximize the system signal-to-noise ratio and resolution and minimize heat generation on the focal plane. In both the linear and binary approaches, the holographic surface-relief pattern is coded to generate a set of local oscillator beams when the relief pattern is illuminated by a single plane-wave. Each beam of this set has the same amplitude shape distribution as, and is collinear with, each single element wavefront illuminating array.

INTRODUCTION

High-resolution infrared laser radars (ref. 1) often suffer from considerable loss of image quality due to speckle noise. This speckle noise is caused by the constructive and destructive interference of wavefronts reflected from a rough target and from the large spatial coherence of the laser radiation source. The only feasible way, at present, to improve the speckle-degraded image quality is to average a number of frames of the scanned image, pixel by pixel. The frame-averaging requirement is for very high scan rates. The use of a detector array reduces this requirement; i.e., it reduces the scan rate while increasing the frame rate.

A problem in high-efficiency heterodyne detection with detector arrays is the loss of heterodyne efficiency due to the misalignment of signal and local-oscillator (LO) wavefronts away from the optical axis when a single uniform local oscillator wavefront is used. The heterodyne efficiency, which is proportional to the vector dot product of the

*This work was sponsored by the Department of the Air Force.

signal (ref. 2) and the local oscillator wavefronts integrated over the entire detector area, decreases rapidly with angular misalignment of signal and LO wavefronts. When this angular misalignment approaches $\theta \approx \lambda/d$ where d is the detector diameter, the detection efficiency falls to approximately zero. This destructive interference imposes a restriction on the maximum number, n, of detector elements in an array with detector separation, s, and at a distance, ℓ, away from a signal exit aperture,

$$n << \frac{\lambda}{d} \cdot \frac{\ell}{s} \tag{1}$$

This type of detection efficiency loss can be alleviated considerably with the use of a cylindrical LO wavefront. Other sources of detection efficiency degradation are mismatches between signal and LO wavefront amplitude distributions and between optimum detector size, d, and the signal diffraction limited Airy spot size. These detection efficiency losses can be quite severe, particularly for telescopes with high obscuration ratio's (see figure 1). Finally the use of a uniform-intensity local oscillator not only reduces the S/N by creating excess LO noise but also generates excess focal-plane heat and lowers the heterodyning system's spatial frequency resolution. Thus, the desirability of an amplitude and angular phase-matched set of LO's is clear.

In our approach, we used a holographic surface-relief grating to generate a set of LO's. A uniform plane-wave of a single LO illuminates the grating so that the reflected light, after passing through the detector focussing lens, consists of a fan of N plane waves focussed on each of the N detectors in the array in phase with the incoming signal (see figure 2). In addition, if the virtual exit aperture calculated for the signal beam path is replaced by a real aperture, then the size of the holographic grating can be chosen to equal or exceed the size necessary to obtain diffraction-limited LO amplitude distributions of the same size as the signal amplitude distribution. The LO amplitude distribution then must have enough spatial frequency bandwidth in the Fourier domain to exceed the spatial frequency bandwidth set by the real exit aperture acting as a low-pass filter. Consequently, the optical signal wavefronts and the LO wavefronts are space-limited by the same low-pass filter and exact signal-to-LO diffraction-limited amplitude matching occurs.

Two techniques were developed to generate the necessary high-accuracy optical-phase relief gratings. The first approach, called the linear or optical technique used the classical concept of holographic recordings in photosensitive materials (positive photoresist). In the recording step, an optical wavefront simulating the LO wavefronts is recorded in photoresist at a blue or near UV wavelength that matches the resist sensitivity. In the reconstruction step, a scaled IR optical wavefront simulating the LO's is generated by reilluminating the recording with an IR (10.6μm) plane wave.

The second approach called the binary or synthetic technique uses a real non-negative coding scheme to generate a complex wavefront with binary π-phase steps deposited on a reflective substrate. When this substrate is

reilluminated with a plane wavefront of the appropriate wavelength, a uniform set of uniform plane LO wavefronts is generated without any need for a previous optical recording.

HOLOGRAPHIC GRATING FABRICATION

The Linear Technique

In the linear (optical) technique (see figure 3), a phase-holographic recording of a reference wavefront and an information wavefront are made in photoresist (AZ 1350-J) with the use of an Argon ion laser beam tuned to 4579 Å. The information beam consists of a set of N plane-waves generated by a scaled metallic mask containing apertures simulating the detector array. Each aperture in the mask acts as a point source that generates a plane-wave by lens Fourier transformation or by propagation, depending on the size of the apertures. The information beam is mixed with a uniform plane-wave at an angle θ_b, and the interference pattern is recorded on a pretreated substrate coated with photoresist (see figure 4). The coherent exposure records the interference pattern in the photoresist by deactivating a photoactive inhibitor compound with a deactivation density proportional to the optic field intensity distribution. In the following resist development step, the light exposure distribution is transformed into a relief pattern at a rate of approximately 1500 Å/sec (ref. 3). The relief depth controls the ultimate diffraction efficiency of the grating (refs. 4 and 5). Because of the mechanical instability of the resist, the relief pattern must be transferred to a mechanically stable and highly reflective substrate. This can be done by ion-beam etching chemical wet etching, or electroplating.

Reillumination of the holographic relief grating with IR light will recreate a set of N uniform plane-wavefronts scaled in angles θ_{IR} and in spatial coordinates X_{IR} in the image domain according to the first-order expressions shown in figure 4. It can be shown that of the Seidel aberrations caused by the mismatch of the three wavefronts, only distortion can not be avoided in Fourier holograms undergoing a wavelength transformation. (ref. 4). However, the positions of the apertures in the object mask simulating the detector array have been calculated and predistorted to compensate for this mismatch.

Typical mask apertures used in these experiments were 8μm in diameter and positioned at approximately 25μm intervals. Position accuracy was better than 1μm. The large wavelength scaling ratio $\lambda_{IR}/\lambda_b \approx 23$ caused the interference angle θ_b to be very small, approximately 1.3°, and required the use of a Mach-Zehnder interferometer recording arrangement with a beam expander and spatial filter in one branch and the metallic mask in the other. Better than $\lambda/50$ optics were used throughout the recording arrangement.

The three problem areas of the technique are (1) substrate reflections, (2) resist deposition flatness quality, and (3) dynamic range of the optic field and resist non-linearities. We chose SKN-5 glass as a substrate material and AR coated the back side with 1/4 λ MgF_2 to avoid the formation of serious interference nodes in the plane of the resist due to reflection from the resist-substrate and substrate-air boundaries. The refractive index of SKN-5 glass closely matches that of AZ-1350J resist ($n \approx 1.675$). Of course, refractive index matching with the liquid glycerol in contact with black chrome can reduce reflections even more. The deleterious effects of substrate reflections are important - - even a 1% residual reflection can cause a 20 or 30% change in developed relief height.

Microfinish and macroflatness are also important for good reconstruction image quality. Microfinish imperfections cause a random relief pattern in the developed photoresist rather than a smooth etching surface and in turn cause a noisy LO background. The deposition of a uniformly thick resist on a one-inch substrate was an extremely difficult problem in our effort to develop high quality (i.e., large array) linear holographic beam formers. To some extent, all our samples exhibited the characteristic doughnut resist spinning profile together with resist redepositions from scattering in the spinner bowl (even in an acetone atmosphere). These nonuniformities are very destructive for holographic recordings where the lowest and incremental spatial frequencies are 0.25 lines/mm.

A third problem concerns the large-intensity dynamic range of the information beam and the limited materials linearity. The material nonlinear distortions have been studied by many researchers (refs. 6 and 7). They are particularly severe in thick resist layers. A coherent superposition of plane-waves leads to a $[\sin Nx / \sin x]^2$ intensity distribution. The minimum dynamic range that needs to be recorded is 23 db. The only feasible way to reduce the dynamic range of the information beam is to introduce randomizing phases in each of the apertures forming the mask. Considering the microscopic size of the mask, this is not an easy task.

Figure 5 shows a single HgCdTe detector scan past the focussed IR(10.6μm) image of a three-element mask that forms a three-beam amplitude-shaped LO. These three LO beams are separated by 530μm, using the magnification of a 12 cm focal length lens, exhibit a very low optical noise background, and produce an optical conversion efficiency of approximately 12%. The width of the LO beams is controlled by the low-pass filtering characteristics of the exit aperture or by the relief hologram's size.

It is our experience that with this technique and its severe limitations of photoresist linearity and large dynamic intensity range of the optic field, a maximum of 8- to 10-high optical-quality LO beams per linear dimension with an arbitrary spatial distribution can be generated. This number of LO's can, of course, be increased somewhat if lower and lower power conversion efficiencies can be tolerated.

The Binary Technique

In the binary (computer lithographic) technique (see figure 3), a grating is formed by a reflective substrate on which a series of small reflective strips separated by an air gap have been deposited. The position and width parameters of these strips can be used to code a complex object wavefront using the phase detour principle in a real non-negative functional form so that the wavefront can be regenerated by optical means.

Our goal is to generate a fan of N uniform plane-waves that are focussed by the system's exit lens onto each of the N elements of a detector array with equal intensity. This approach requires a Fourier superposition of plane-waves of the form,

$$\frac{1}{N} \sum_{n=1}^{N} A_o \, e^{2\pi j n \alpha x} \tag{2}$$

where the propagation vector $k = 2\pi\alpha$ is determined by the detector configuration and the focal length, f, of the lens. That is,

$$\lambda f \alpha = d + s \tag{3}$$

where d + s is the detector spacing (see figure 6). The system's exit lens focal length is in turn determined by the necessary signal and LO spot sizes to be matched to the detector size, i.e.,

$$\frac{2.44\ \lambda f}{D} \approx 0.75\ d \tag{4}$$

for a grating size of diameter D. The combination of expressions 3 and 4 yields a spatial frequency of $\alpha \approx 0.437\ 10^{3}$ 1/meter from our system parameters.

To avoid overlap with the strong undiffracted beam components, this collection of plane-waves must be placed on a spatial carrier frequency that diffracts the light at an angle β. This carrier frequency (or equivalently, diffraction angle) must be chosen judiciously so that no signal aliasing occurs between the different diffraction orders, yet must be large enough so that the fringe periodicity is not limited by the pattern generator resolution. From a simplified analysis outlined in figure 6, one can determine that for a diffraction angle β of only a few degrees, the fringe accuracy over a 750 mils holographic grating must be in the order of 500 Å if a 10% LO misalignment can be tolerated. This is a very high accuracy requirement.

There is, however, another choice: the grating carrier frequency of period T can be changed from either parallel (x direction) to or orthogonal (y direction) to the carrier frequency 1/T. After the orthogonal placement of carrier and information spatial frequencies, β_{max} equals $N\alpha/2$, and the grating tolerance is greatly relaxed to an accuracy of a few μm over the holographic surface.

The required phase of the LO wavefront $\phi(y)$ can, therefore, be described by

$$e^{j\phi(y)} \sim \sum_{n=-N/2}^{N/2} e^{2\pi jn\alpha y} \tag{5}$$

or

$$e^{j\phi(y)} \sim [1 + 2 \sum_{n=1}^{N/2} \cos 2\pi n\alpha y]$$

Unfortunately, the phase $\phi(y)$ that describes the plane-wave superposition cannot be extracted in real form for substitution in a phase detour equation. This problem can be remedied by creating a composite grating of period T and shifting its reflection by a phase $\exp(j\pi/2)$ or, equivalently, a T/2 period. If this plane-wave distribution generated by the composite grating is equated to the required superposition of plane-waves, one finds the holographic phase modulation $\phi(y)$ of each fringe, i.e.,

$$\phi(y) \sim \sin^{-1} [m(\frac{1}{2} + \sum_{n=1}^{N/2} \cos 2\pi n\alpha)] \tag{6}$$

where m is proportional to the modulation depth of the fringes.

The dynamic range of this phase distribution and that of the generated optic field can be reduced considerably by introducing a randomizing phase factor $\exp(j\psi_n)$ to each of the plane-waves in N/2 conjugate pairs,

$$\phi(y) = \sin^{-1} [\frac{m}{\sqrt{2N}} (\frac{1}{2} + \sum_{n=1}^{N/2} \cos(2\pi n\alpha y + \psi_n))] \tag{7}$$

In our system, we have chosen a deterministic binary phase code (ref. 8), $\psi_n(0,0,0,\pi,0,0,\pi,0)$ that yields a dynamic range reduction of at least $(\sqrt{2N})^{-1}$. Many other binary and polyphase codes exist (ref. 9) that bound the amplitude dynamic range of a plane-wave superposition. This randomizing phase factor has the same effect as introducing microscopic phase plates in the mask apertures in the optical technique. It simply randomizes the phases between the LO's but maintains a constant phase over each detector surface.

Each plane-wave component of this sum, therefore, interferes with the incident reference wavefront $\exp(2\pi j\, x/\lambda \sin\beta)$. Using the Bragg condition, the reference wavefront is $\exp(2\pi j\, x/T)$. The resulting interference forms a fringe pattern that satisfies the following periodic equations (phase detour principle):

$$x = \frac{-\phi(y)}{2\pi} T + nT$$

$$x = \frac{\phi(y) + \pi}{2\pi} T + nT \qquad (8)$$

where T is the periodicity or distance between two homologous points along the grating. A partial, strongly aberrated, visible-light (HeNe) reconstruction of a 17-element LO array is shown in figure 7.

A high resolution pattern generator uses equation (7) to generate a hologram large enough to satisfy the required space-bandwidth product by repeatedly plotting the fringe pairs of equations (8). The holographic patterns were initially generated at 5X magnification on a Kodak emulsion plate using a Mann 1600-A pattern generator. The building block rectangle size was 38 x 2 mils with 0.5 mil accuracy on a 5X reticle. In order to use a pattern generator with this limited accuracy we had to enhance its accuracy and resolution artificially. This was done by plotting a reticle of a single square holographic unit cell and by a 5X photoreduction. Then with a step-and-repeat process, the hologram was built up of these unit cells to its diffraction-limited size. Another 5X photoreduction brought the mask down to its final size while maintaining the absolute spatial frequency of the grating. This process, of course, also reduced pattern generation time considerably to approximately 8 1/2 hours.

The resulting phase quantization of the highest image spatial frequency component was 80 and the amplitude quantization was 20. The effects of these quantizations are difficult to analyze (ref. 10). If, however, the quantization errors are assumed to be uniformly random, then it can be shown that optimum-magnitude quantization depends on the number of phase quantizations, N_p, via $[\sin(\pi/N_p)/(\pi/N_p)]$, i.e., amplitude-phase coupling between errors exists (ref. 11).

After completion of the pattern in the primary emulsion mask it is replicated in thin positive resist on a chrome-coated conformable mask and is chemically etched. A photograph of a section of such a mask is shown in figure 8. The period between two homologous points in the x direction (vertical) is 2 mils, whereas the y direction (horizontal) carries the information, i.e., the phase modulation $\phi(y)$. The final substrate is then coated with thick resist (approximately 1/4 $\lambda \cos\theta$, where θ is the angle of incidence) and is exposed through this conformable mask in intimate contact and is developed. The close contact is essential to avoid degradation of the thick resist side-walls and to maintain the high

acuity. Ion beam bombardment of the relief surface transfers the developed resist pattern into a stable substrate. The ion beam etching applies to both linear holograms (where the resist is not developed away down to the substrate) and binary holograms (where it is). By choosing a suitable substrate with a high ion-beam-etch ratio compared to the resist, we can take advantage of the resist-substrate-etch magnification ratio, i.e., AZ1350:ST-quartz:Poly-GaAs = 150:279:575 Å/min. The cleanup of the residual resist and organics was performed by immersing the sample in a plasma of 97% He and 3% O_2. Figure 9 shows these processing steps for both the linear and binary techniques. A final 800 Å chrome-gold coating provides the needed reflection for efficient power conversion (see figure 10).

These binary gratings were also tested by scanning the focussed first-order diffracted wavefront with a single HgCdTe detector obscured by a 10μm pinhole. The result of this one-dimensional scan of the 17-element LO beam profile is shown in figure 11. The LO beams were separated by 112μm, consistent with the detector separation in the array. They exhibited low optical background noise. The orientation and periodicity (T = 3 mils) of this grating were chosen such that a 90° relationship existed between the incident wave and the first diffraction order. The nonuniformities between the different LO elements are assumed to be due to the inaccuracies in the step-and-repeat process that generated the grating from the individual unit cells. This step-and-repeater had a position accuracy of only 0.5 mils (approximately one wavelength) and imposed a periodic modulation on the LO amplitudes, whereas the low amplitude of the center LO was traced to a mathematical error in the program that generated the mask.

DISCUSSION

We have shown the feasibility of generating a set of LO's that are matched in amplitude distribution and angular phase with the incident signal wavefronts on 1- or 2-D detector arrays with the use of holographic relief gratings by two different techniques.

The number of LO's that can be generated with linear holograms in the optical technique is limited by the high dynamic range of the optic field and by resist linearity. Therefore, this technique, although useful, is restricted to small detector arrays (a maximum of 10 detectors per linear dimension) such as symmetrical detector configurations used for tracking purposes.

The binary technique has its limitations also, even though it eliminated or reduced the problems of substrate reflections, resist flatness, and dynamic range that hampered the optical technique. The major problems with the binary technique are pattern generator accuracy, resolution, and generation time. In addition, at high diffraction angles or low periodicities the fringe duty cycle and the phase modulation depth must be reduced more and more. When the fringe spacing becomes comparable to the wavelength

(i.e., < 5λ), the concept (in terms of constructive interference of waves that are specularly reflected) on which this theory is based no longer applies to surface dimensions comparable to the wavelength of the illuminating light. For instance, in figure 8, a picture of an earlier mask with $T \approx 50\mu m$, m = 1 and 20% fringe duty cycle (i.e., T/10 fringe width), we still observed strong polarization effects, resonances, and possibly surface plasmon effects (ref. 12). Reducing the grating periodicity and phase modulation range unfortunately also reduces the diffraction efficiency. The coding method we have discussed is by no means the only or most efficient one. Many more elaborate codes exist (ref. 13). It seems feasible to illuminate a 100-element heterodyning linear detector array with LO beams from a single binary grating with reasonable power efficiency.

REFERENCES

1. R. J. Hull and S. Marcus, Proceedings of IEEE National Aerospace and Electronics Conference, Dayton, Ohio, 662 (May 1978).

2. D. Fink, Appl. Opt. 14, 689 (1975).

3. S. Norman and M. Singh, Appl. Opt. 14, 818 (1975).

4. H. Smith, Principles of Holography, Wiley-Interscience (1969).

5. R. Bartolini, Appl. Opt. 13, 129 (1974).

6. M. Beesley and J. Castledine, Appl. Opt. 9, 2720 (1970).

7. A. Neureuther and F. Dill, Proceedings of Symposium on Optical and and Acoustical Micro-Electronics, Polytechnique Institute of New York, 223 (April 1974).

8. W. Rudin, Proc. of Am. Math, Soc 10, 855 (1959).

9. H. Akahori, Appl. Opt. 12, 2336 (1973).

10. R. Gabel and B. Lui, Appl. Opt. 9, 1180 (1970).

11. W. Dallas, Appl. Opt. 13, 2274 (1974).

12. K. Utagawa, J. Opt. Soc. Am. 69, 333 (1979).

13. C. Hsueh and A. Sawchuk, Appl. Opt. 17, 3874 (1978).

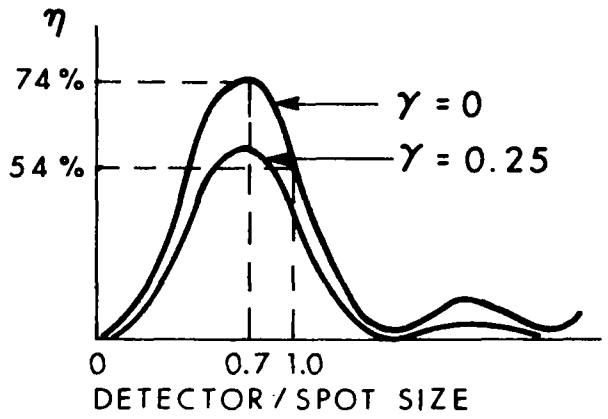

(a) Uniform LO illumination.

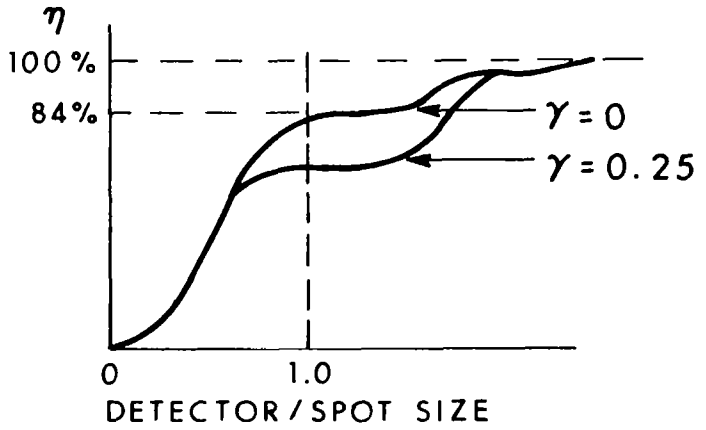

(b) Amplitude shape matched LO illumination.

Figure 1.- Heterodyne efficiency as a function of detector/signal-spot-size ratio.

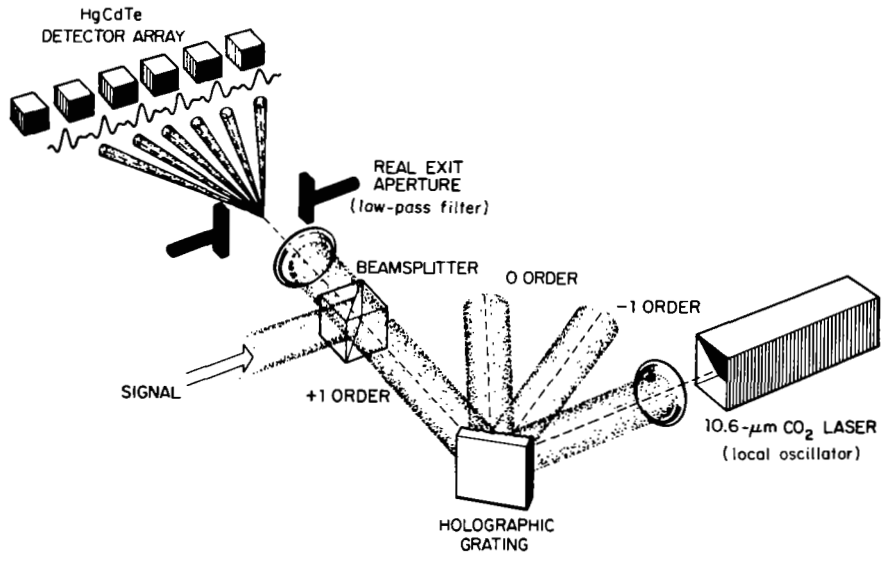

Figure 2.- Holographic generation of a multibeam local oscillator.

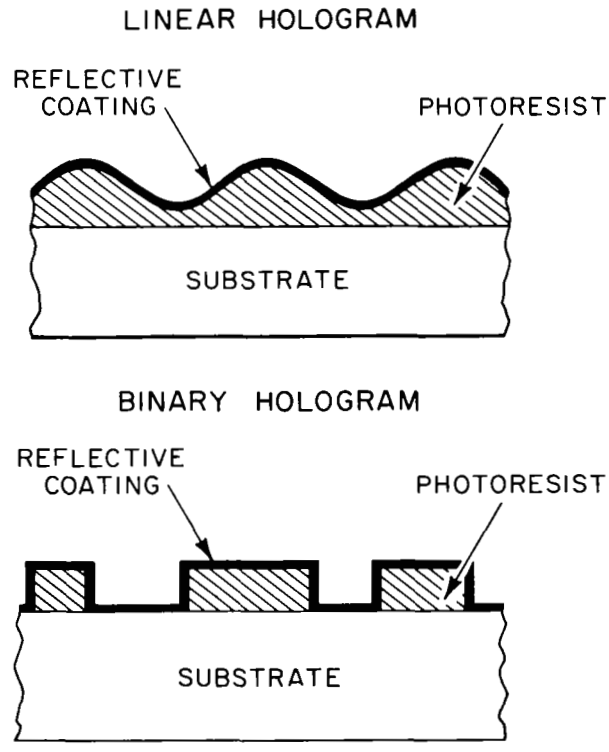

Figure 3.- Characteristics of linear and binary reflection holograms.

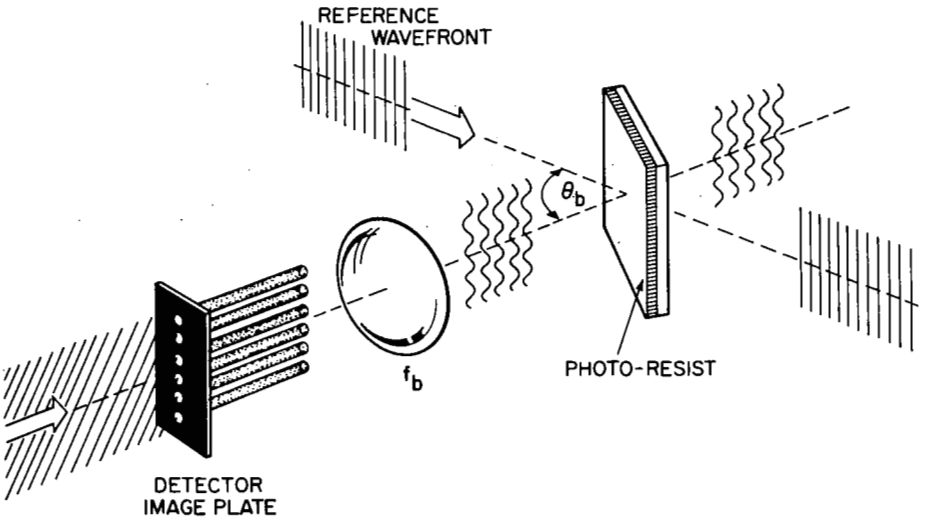

$$\text{TO FIRST ORDER:}\quad \theta_{IR} = \frac{\lambda_{IR}}{\lambda_b}\,\theta_b$$

$$X_{IR} = \frac{\lambda_{IR}}{\lambda_b}\cdot\frac{f_{IR}}{f_b}\cdot X'_b$$

Figure 4.- Formation of a linear holographic grating.

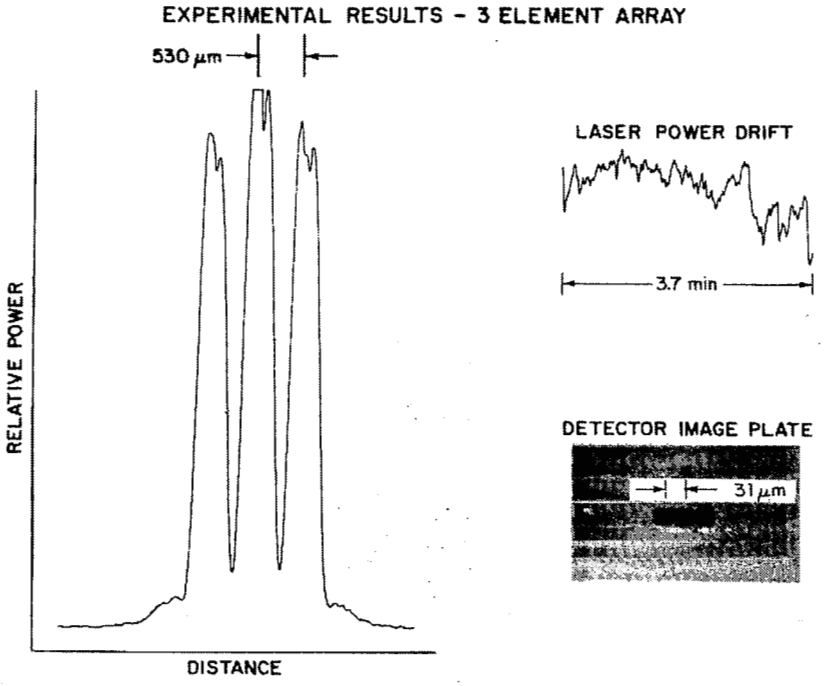

Figure 5.- An intensity scan past a three-element IR (10.6μm) local oscillator generated by a linear holographic grating.

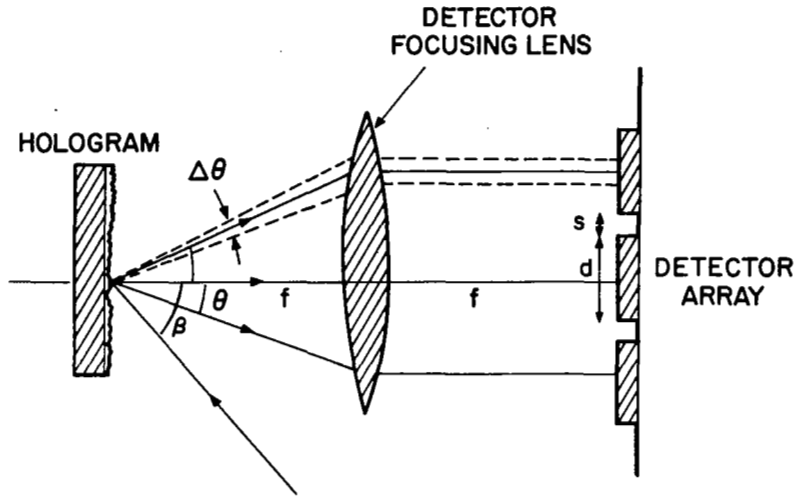

$$\text{GRATING LAW: } T = \frac{\lambda}{\sin\beta}$$

$$\text{GRATING TOLERANCE: } \Delta d_s = \frac{\cos\beta}{(\sin\beta)^2} \cdot \lambda \cdot \Delta\theta$$

$$\text{L.O. ALIGNMENT } \Delta\theta \leq \widehat{\tan}\left[\frac{d+s}{10f}\right]$$

Figure 6.- LO alignment dependence on fringe position accuracy.

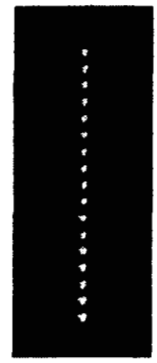

Figure 7.- A strongly magnified, aberrated, visible light (HeNe) reconstruction of a 17-element LO beam from a binary grating.

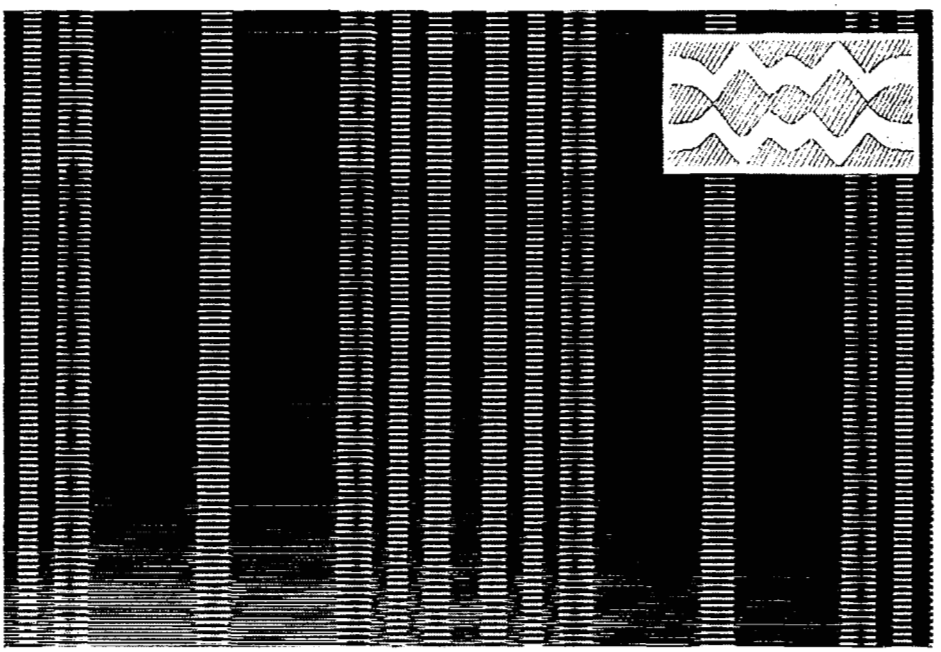

Figure 8.- Enlarged photograph of a section of a binary mask, T = 50μm, m = 1. The insert shows a section of a compressed conjugate fringe pair.

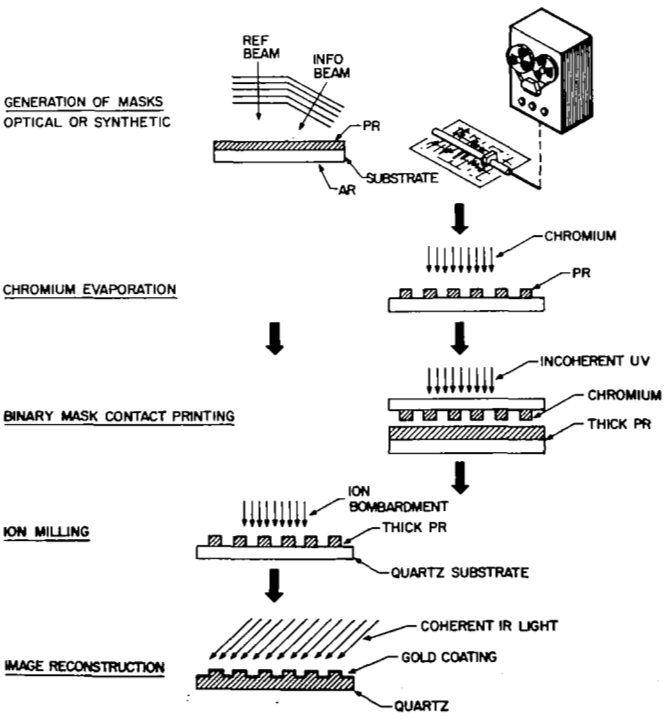

Figure 9.- Processing steps in the formation of linear and binary relief gratings.

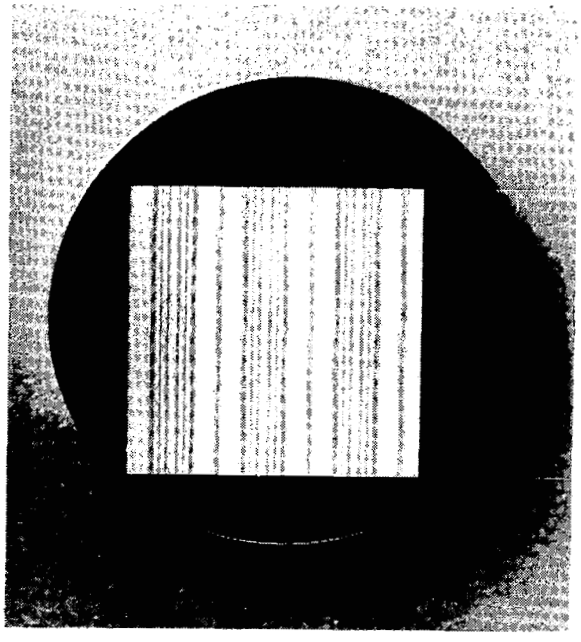

Figure 10.- A photograph of a 3/4 inch gold coated binary holographic grating on a poly-GaAs substrate.

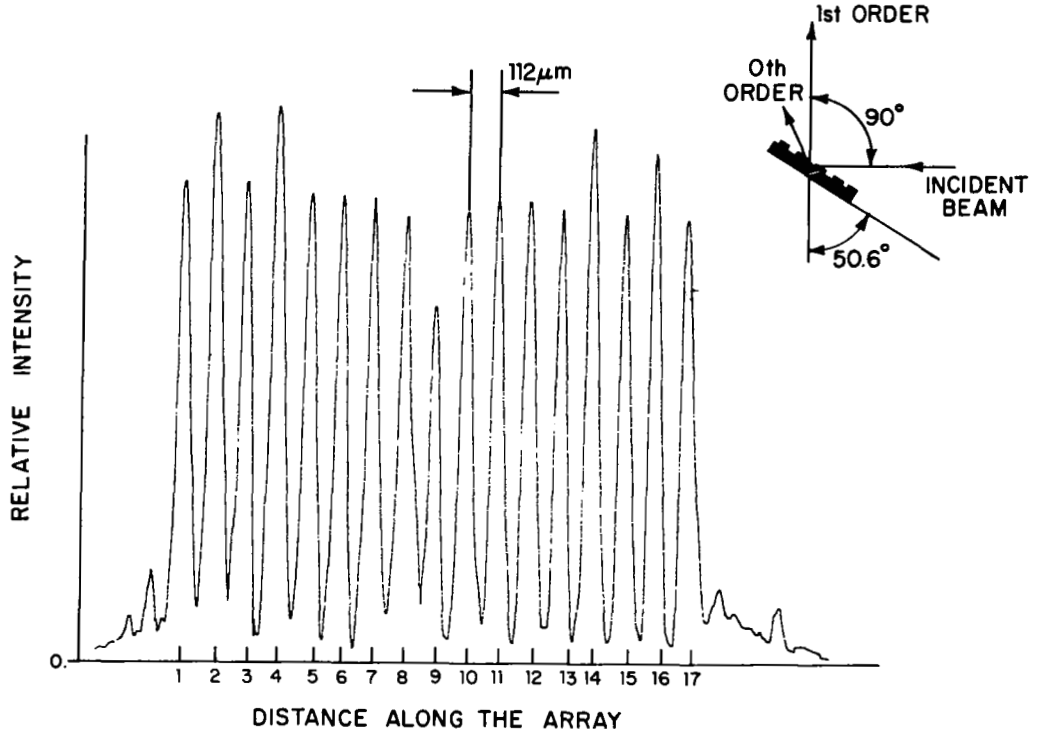

Figure 11.- An IR (10.6μm) detector scan past a focussed wavefront generated by a 17-element holographic binary grating.